Unsupported planar lipid membranes formed from mycolic acids of *Mycobacterium tuberculosis*

Kyle W. Langford, Boyan Penkov, Ian M. Derrington, and Jens H. Gundlach[1]

Department of Physics, University of Washington, Seattle, WA 351560

Abstract   The cell wall of mycobacteria includes a thick, robust, and highly impermeable outer membrane made from long-chain mycolic acids. These outer membranes form a primary layer of protection for mycobacteria and directly contribute to the virulence of diseases such as tuberculosis and leprosy. We have formed in vitro planar membranes using pure mycolic acids on circular apertures 20 to 90 μm in diameter. We find these membranes to be long lived and highly resistant to irreversible electroporation, demonstrating their general strength.▪ Insertion of the outer membrane channel MspA into the membranes was observed indicating that the artificial mycolic acid membranes are suitable for controlled studies of the mycobacterial outer membrane and can be used in nanopore DNA translocation experiments.—Langford, K. W., B. Penkov, I. M. Derrington, and J. H. Gundlach. **Unsupported planar lipid membranes formed from mycolic acids of *Mycobacterium tuberculosis*.** *J. Lipid Res.* 2011. **52:** 272–277.

With nearly two million yearly deaths caused by infections of *Mycobacterium tuberculosis* (1) and with more than 200,000 people debilitated by infections of *Mycobacterium leprae* (2), there is concerted need to understand the mechanisms of Mycobacterial resilience. Part of the persistence and lethality of these diseases is due to the impermeable mycobacteria cell wall. Mycobacteria, including *M. tuberculosis,* have developed strains that resist contemporary multi-drug treatment regimes (1). Mycobacteria's unique ∼8 nm thick outer cellular casing (3) has far lower permeability to hydrophilic agents than *Escherichia coli*'s cell wall and is a key factor in the drug and environmental resistance of mycobacteria (4).

Although containing other constituents, the mycobacterial outer membrane contains 30–40% mycolic acids (MAs) by mass (5, 6). MAs contain a carboxylic acid headgroup with two hydrophobic tails of unequal length (**Fig. 1**). One tail is a long meromycolate chain containing 50 to 70 carbon atoms with cyclopropane rings, ketones, methoxy groups, and/or double bonds. The shorter α-branch contains ∼25 carbons and is a straight chain alkane. The meromycolate tail is ∼8 to ∼11 nm when stretched and likely requires a unique arrangement of the lipid tails to form the 8 nm thick in vivo membrane; the arrangement of the fatty acid chains in the two leaflets of the membrane is a subject of discussion (3, 7, 8). In vivo, the mycolic acids are covalently linked by the carboxolate group to arabinogalactan or trehalose sugars (4, 9). The significant impermeability of the mycobacterial membranes results in the need for pathways for hydrophilic solutes. This pathway is mediated by protein pores (7).

In vivo studies of pore proteins in the mycobacterial cell-wall of *Mycobacterium smegmatis*, a close relative of *M. tuberculosis* (10, 11), led to the discovery of the outer membrane pore *Mycobacterium smegmatis* porin A (MspA). In *M. smegmatis* (12), MspA is the most abundant protein and forms the primary pathway for hydrophilic nutrients to traverse the outer membrane (13, 14). Other membrane porins such as OmpATb and iron transporters have been isolated in mycobacterium species but their behavior in their natural environment remains unexplored (7, 15, 16).

Our interest in MspA arose because of the pore's unique geometry and stability, which make it an excellent tool for single molecule studies and, in particular, MspA's application to nanopore DNA-sequencing (17, 18). To use such a transmembrane pore for DNA sequencing (17), a voltage is applied across the pore to draw individual charged DNA molecules through the pore. As the DNA passes through the pore, the ion current that also flows through the pore provides information about the DNA's sequence. A robust membrane is required to form long-lasting experimental setups or to construct practical devices. In an effort to find a membrane with enhanced stability, we formed mem-

Abbreviations: DPhPC, dipalmitoylphosphatidylcholine; MA, mycolic acid; MspA, *Mycobacterium smegmatis* porin A.
[1] To whom correspondence should be addressed.
   e-mail: jens@phys.washington.edu

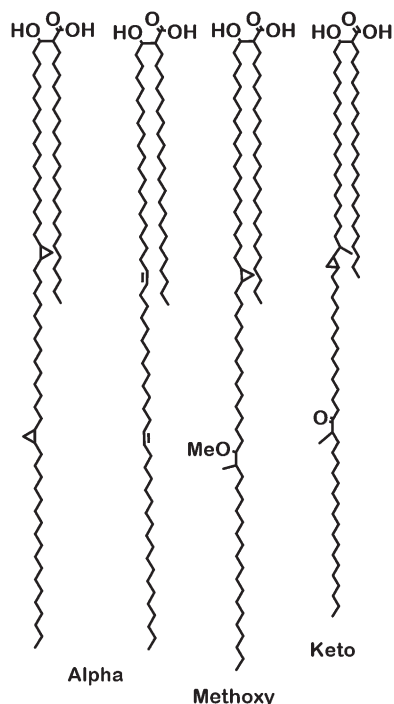This article is available online at http://www.jlr.org

Fig. 1. Chemical structure of the dominant mycolic acids present in mycobacterial outer membranes (4).

branes from MA to more closely mimic MspA's natural membrane environment.

In this paper, we demonstrated planar membranes formed in vitro using MAs. We found that the artificial MA membranes have very long lifetimes and, when compared with dipalmitoylphosphatidylcholine (DPhPC) membranes, withstand higher voltages before rupturing. Finally, we found that MspA forms transmembrane channels in the MA membranes with the same characteristics as MspA in DPhPC membranes.

MATERIALS AND METHODS

Apparatus

The experimental setup has been described previously (19, 20). Briefly, a 20-90 μm Teflon aperture was formed by melting Teflon heat shrink tubing (Small Parts, Inc.) around a finely sharpened needle or a wire. After removing the needle or wire, the tubing was cut to form an aperture of the desired width. The tubing was then bent to connect two ∼200 μl wells in a Teflon holder. Ag-AgCl electrodes were used to ground the resultant *cis* well and connect the *trans* well to either an Axopatch 200B, 1B or 1C patch clamp amplifier operated in voltage clamp mode. To find the membrane rupture voltage of the MA membranes, which exceeded the 1.2 V maximum output voltage of the patch clamp amplifiers, we instead used a variable power supply in series with a Keithley 485 picoammeter. A 1.0 M KCl solution in DI water, buffered to pH $8.0^{+/-}$ 0.05 with 10 mM HEPES, electrically connected the two wells.

Ion channel currents were sampled at 250 kHz or 500 kHz and low-pass filtered with a 4-pole Bessel filter at 1/5 the sampling rate. Data acquisition was controlled by custom software written in LabWindows and LabVIEW. For lifetime measurements, data were sampled at 10 Hz.

Membrane formation. We purchased mycolic acids (≥98%, Sigma-Aldrich, St. Louis, MO) (21) that were extracted from *M. tuberculosis* and were dissolved in chloroform to 50 g/L and stored at −20°C until use. The mycolic acid membranes were formed using the painting technique, widely used in similar experiments with DPhPC (19). The process began with two preparatory steps. In the first step, the Teflon aperture was pretreated with a coat of a lipid-hexane mixture. One microliter of the MA/chloroform solution was air dried in a glass test tube, then resuspended in 0.01 g hexane. One microliter of the resuspended MA pretreating solution was applied to *cis* side of the Teflon aperture and then gentle air pressure was applied with a syringe from the *trans* side to clear the aperture as the hexane evaporates. After clearing the solution from the aperture once, another 1 μl of pretreating solution was applied and cleared. After allowing the system to air dry for 15 min, an electrical connection between the two electrodes was established by putting the KCl buffer in the aperture, tube, and the wells.

In the second preparatory step, the lipid was painted on the aperture. Ten microliters of the MA/chloroform solution was air dried on a chloroform-cleaned glass slide. Then, ∼0.1 μl hexadecane was applied onto the MA and the solution was heated to 35°C for ∼5 min to promote incorporation of the hexadecane into the lipid. When the MA-hexadecane mixture reached a gel-like consistency, an ∼0.1 mm diameter blob of the mixture is applied to a single bristle brush. While monitoring the ion current through the aperture, the lipid-solvent mixture was gently applied over the Teflon aperture until the current falls to zero. Manually forcing buffer through the aperture from the *trans* side eliminated the physical blockage. For apertures greater than 40 μm in diameter, the lipid was applied to the outer edge of the aperture rather than over the top of the aperture.

The membrane was formed by placing a 3–6 μl air bubble over the prepared aperture using a micropipette and then the air bubble was gently retracted. Membrane formation was indicated by the current through the aperture sharply falling to zero. If trans-membrane pores can form within the lipid system, we assume the presence of a bilayer membrane and not a multi-lamellar lipid structure or a physical lipid obstruction. Observation of these pores is described below.

MspA channel measurements. The concentration of MspA (M1-NNN-MspA) (22) in single channel experiments was 0.04 μg/ml in 0.01% wt/v Genapol and DI-water; the concentration for multi-channel experiments was 0.4 μg/ml in 0.1% wt/v Genapol. From this solution, ∼1 μl was added to the 100-200 μl of the *cis* volume above a MA membrane and then mixed thoroughly. The MA membrane was reformed with the air bubble technique, described above, after which we observed stepwise conductance changes corresponding to pore insertion (**Fig. 2**). If a conductance appropriate for a single channel was measured, we rapidly perfused the protein solution in the *cis* well with the working buffer to avoid the insertion of further channels.

pH measurements. We examined the stability of the membranes in the presence of alkaline and acidic conditions from pH 2 to pH 12 by replacing the 1M KCl pH 8.0-buffer on the *cis* side with different 1M KCl solutions buffered between pH 2 to pH 12. The solution at pH 8 was buffered with 10 mM HEPES, whereas the other solutions were buffered with an appropriate mixture of 40 mM CH_3COOH, boric acid, and K_2HPO_4. The pH of the various buffers was measured using an Orion perpHecT logR meter with a Beckman electrode calibrated in the appropriate pH range.
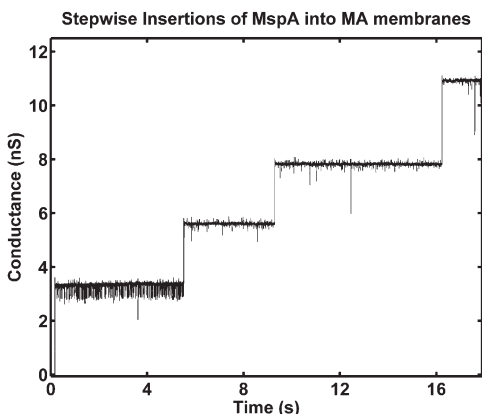
Fig. 2. Change in conductivity across MA membranes with discrete current steps after the addition of MspA. The observed current steps are indistinguishable from current levels observed in DPhPC membranes.

RESULTS AND DISCUSSION

Membrane formation

The MA membranes were formed with similar reliability to DPhPC membranes. Also, MspA incorporated similarly into both MA and DPhPC membranes at ~0.2 pores/second with a concentration of ~10 nM MspA. The MspA pores in the MA membranes lasted for several h before spontaneously leaving the membrane, similar to the behavior of MspA pores in DPhPC membranes.

MspA has a height of ~9 nm and a hydrophobic length of only ~5 nm that limit the hydrophobic barrier size that the pore can penetrate. In vivo, the outer membranes of Mycobacteria are ~8 nm (3, 8). If the membrane consisted of two lamella of MA (with an oil layer separating the two), MspA would be unable to span the membrane. Therefore, the insertion of the transmembrane MspA pore within the MA system strongly suggests the formation of bilayer membranes instead of other lipid configurations.

Membrane resistance, rupture, capacitance, and longevity

We examined MA membranes using the Axopatch amplifier to determine a lower bound of their resistance. On the 20-40 μm apertures, the measured ion current was <1 pA when ±1.2 V was applied across the membrane, corresponding to >1 TΩ resistance. DPhPC membranes formed on the same apertures also exhibited resistance values >1 TΩ.

To determine the rupture voltage of MA and DPhPC membranes, the applied voltage was ramped at about 100 mV/s until the current across the membrane increased abruptly at the rupture voltage, V_{rup}. The membrane was then reformed by application of another air bubble and the procedure was repeated. The histogram of the rupture voltage is presented in **Fig. 3**. For MA membranes, we found an average rupture voltage of V_{rup_MA} = 2.0 V with a standard deviation of 0.7 V (N = 330). For comparison, we formed DPhPC lipid membranes on the same apertures and with the same operating conditions and found V_{rup_DPhPC}= 0.50 V with a standard deviation of 0.09 V (N = 209). Because the MA membranes withstood relatively high applied voltages, a

BK Precision 875b capacitance meter could be used to measure their capacitance. For Teflon apertures with diameters between 56 μm to 85 μm, the largest on which membranes could still be formed, we found capacitance values ranging from 0.9 to 2.8×10^{-3} F/m^2, indicating average thicknesses between 7 and 22 nm (dielectric constant ε_r= 2.3). These thicknesses are consistent with the membrane thickness found in vivo of ~8 nm. We attribute the large range of thickness to several factors including the uncertainty of the actual area of the membrane and the unknown extent of solvent incorporation into the membrane. Immediately after membrane formation, the capacitance rose toward an asymptotic value with a time constant of ~5 min. Such increase in capacitance is consistent with bilayer formation observed with DPhPC lipids (23).

We examined the lifetimes of MA membranes by monitoring the conductance of membranes formed with MspA pores. We left these membranes with 200 mV applied until we terminated the experiments after more than 3 days (N = 4). This puts a lower bound on the MA membrane lifetime at 3 days, significantly larger than the longest lifetime of 1 day we observed with DPhPC membranes.

pH influence on membrane stability

The MA membranes could be formed and reformed with buffer of pH 2 to pH 9 presented to their *cis* side. The membranes survived at each pH for at least 20 min. At pH as low as 2, the membrane could be readily reformed and pores inserted successfully. Above pH 9, membrane formation was compromised, but bringing the buffer back to a pH of <7 restored membrane formation and stability. The membrane stability was monitored by measuring the ion current. The presence of a measureable current with 200 mV applied, as seen above pH 9, indicated formation of leaks and a significant decrease in bilayer stability.

Single MspA channel measurements

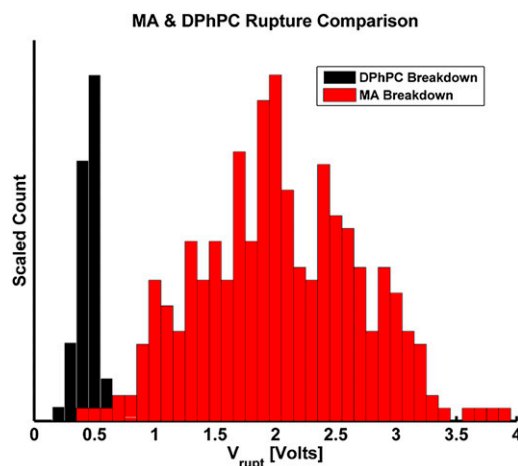To demonstrate that the MspA incorporated in MA were proper trans membrane channels, we measured their I-V

Fig. 3. The scaled histograms of rupture voltages of MA membranes (N = 330) and DPhPC membranes (N = 205) includes data from several different ~20 μm apertures. MA membranes were confirmed via insertion of MspA proteins after rupture experiments.

curves and conducted DNA translocation experiments. The I-V curves of MspA exhibit the same quantitative characteristics as those of MspA in DPhPC membranes (**Fig. 4**) indicating that MspA is able to span the membrane and that the inner channel of MspA was not appreciably affected by its membrane environment. In order to further insure the channel integrity and the usefulness of the MA-MspA combination for nanopore sequencing, we conducted DNA translocation experiments. We repeated experiments that we had previously carried out with single MspA channels in DPhPC membranes (18). Because single-stranded DNA translocates too rapidly (>1 nt/µs) to observe well-characterized current signatures, we used a DNA hairpin that could not complete translocation until the double-stranded section dissociated. During this brief pause the single-stranded section of the hairpin DNA held in MspA's constriction yields well-resolved ion current levels. These current levels were characteristic of the nucleotides residing at the constriction (**Fig. 5**). We carried out experiments with a poly-dA DNA hairpin tail sequence and found the ion current levels to be indistinguishable from analog experiments with MspA in DPhPC membranes (**Fig. 6**).

Fig. 5. A stylized version of MspA is shown here in a nondescript membrane; the duplex DNA is unable to thread through the pore's smallest constriction. Image not to scale.

DISCUSSION

MA membranes exhibit more stability than comparable DPhPC membranes

Our experiments demonstrate the first unsupported membrane established in vitro made from MA. In comparison with DPhPC membranes, we find that MA membranes withstand considerably larger voltages before rupturing. A number of factors influence the stability of membranes (24–27). The MA and DPhPC membranes have significantly different melting temperatures; M. *tuberculosis* cell wall extracts have been found to change phase as high as 63°C, whereas DPhPC has no known phase change (28, 29). Thus, we conclude the rem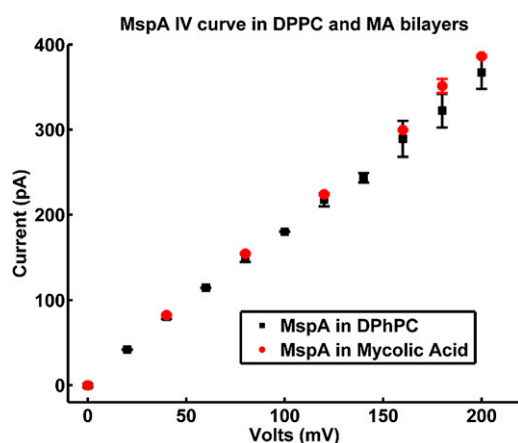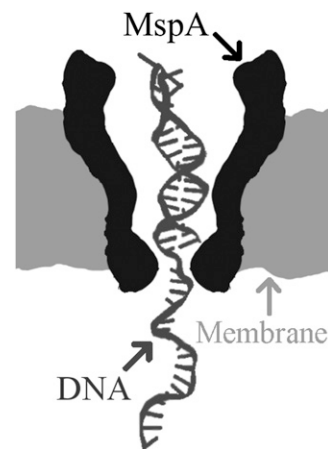arkable robustness of MA membranes must be attributed to the structure and interactions of MA's constituent lipid chains.

MA and DPhPC molecules differ significantly in the chemical structures of the lipid headgroups and tails. Liu et al. (30) demonstrated the importance of the lipid chain length in in vivo studies with mutated *M. smegmatis* that were unable to synthesize full-length MAs. In comparison to membranes from full-length MA in wild-type *M. smegmatis*, the membranes of the mutated populations were found to be more permeable to hydrophobic agents (30, 31). The importance of chain length is also seen in phospholipid membranes, where the permeability of charged ions increases (32) and mechanical strength (33) decreases with small decrements of the hydrophobic chain length. Although the negatively charged MA headgroup is substantially different than the zwitterionic DPhPC head-
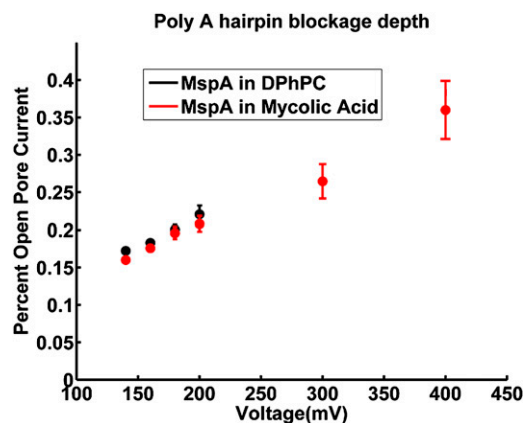

Fig. 4. Shown is a comparison of MspA I-V curves in MA and DPhPC membranes. At negative voltages MspA gating in both membranes obscures the open state current and is omitted. For MspA in DPhPC membranes N = 9 pores, for MspA in MA, N = 2.

Fig. 6. Displayed are the ion current blockage levels caused by homo-polymer adenine hairpin tails temporarily held in a MspA pore embedded in an MA or DPhPC membrane. The current is expressed as fraction of the open state current at the given voltage. At voltages above 200 mV, DPhPC membranes become too fragile for extended experimentation, whereas MA membranes allow measurements at much higher voltages. The duration of events recorded above 400 mV were too short to confidently extract a characteristic ion current.

Mycolic acid unsupported membranes   275

group, neither form hydrogen bonds at pH 8, suggesting that the headgroup is unlikely to account for the rupture voltage differences (34). Thus, the size and configuration of the MA tails and associated thickness of the resulting membranes appear to be the determinant cause of the stability of the MA membranes. In particular, the assembly of MA lipid tails within the membranes may play a significant role in the membrane's function (7). Artificial MA membranes are useful for the closer examination of the mycobacterial outer membrane.

Trans-membrane pores in MA membranes

The influence of the membrane on pore formation, conformation, and function is an unanswered question of interest in drug development and in understanding the folding mechanics of porins (35). For the channel MspA in MA and in DPhPC membranes, we find that the open-channel current exhibits identical conductance and rectification. Furthermore, we observe identical DNA translocation properties through MspA in the two membranes. These conductance and DNA translocation properties are highly sensitive to the structure of MspA (18, 20). Hence, our observations suggest that the substantial difference between membranes composed of MA and DPhPC does not appreciably alter the trans-membrane conformation and function of MspA channels.

CONCLUSIONS

We have formed unsupported artificial planar membranes from MAs extracted from *M. Tuberculosis*. The ability to construct in vitro MA membranes may provide a new tool to examine the arrangement and configuration of the MA lipids in a membrane. Furthermore, the in vitro MA membranes permit the controlled examination of drugs and chemicals through outer membrane pores found in mycobacterial outer membranes such as MspA, OmpATb, and possibly Rv1689 (36). Such examination may help to improve treatment of mycobacterial infections.

Beyond research in mycobacteria, these MA membranes may provide a building block for bio-nanotechnological applications that rely on the stability of lipid membranes (18). These include next-generation nucleic acid sequencing and nanopore force spectroscopy.

REFERENCES

1. World Health Organization. 2009. Global Tuberculosis Control: a short update to the 2009 report. *In*. World Health Organization, Geneva, Switzerland.
2. World Health Organization. 2007. Global Leprosy Situation, 2007. *Wkly. Epidemiol. Rec.* **82:** 225–232.
3. Hoffmann, C., A. Leis, M. Niederweis, J. Plitzko, and H. Engelhardt. 2008. Disclosure of the mycobacterial outer membrane: cryo-electron tomography and vitreous sections reveal the lipid bilayer structure. *Proc. Natl. Acad. Sci. USA.* **105:** 3963–3967.
4. Brennan, P. J., and H. Nikaido. 1995. The envelope of mycobacteria. *Annu. Rev. Biochem.* **64:** 29–63.
5. Rastogi, N., E. Legrand, and C. Sola. 2001. The mycobacteria: an introduction to nomenclature and pathogenesis. *Rev. Sci. Tech.* **20:** 21.
6. Barry, C. E. 2001. Interpreting cell wall 'virulence factors' of Mycobacterium tuberculosis. *Trends Microbiol.* **9:** 237–241.
7. Niederweis, M., O. Danilchanka, J. Huff, C. Hoffmann, and H. Engelhardt. 2010. Mycobacterial outer membranes: in search of proteins. *Trends Microbiol.* **18:** 109–116.
8. Zuber, B., M. Chami, C. Houssin, J. Dubochet, G. Griffiths, and M. Daffe. 2008. Direct visualization of the outer membrane of mycobacteria and corynebacteria in their native state. *J. Bacteriol.* **190:** 5672–5680.
9. Zhang, J., K-H. Khoo, S-W. Wu, and D. Chatterjee. 2007. Characterization of a distinct arabinofuranosyltransferase in *Mycobacterium smegmatis. J. Am. Chem. Soc.* **129:** 9650–9662.
10. Niederweis, M., S. Ehrt, C. Heinz, U. Klocker, S. Karosi, K. M. Swiderek, L. W. Riley, and R. Benz. 1999. Cloning of the *mspA* gene encoding a porin from *Mycobacterium smegmatis. Mol. Microbiol.* **33:** 933–945.
11. Trias, J., V. Jarlier, and R. Benz. 1992. Porins in the cell wall of mycobacteria. *Science.* **258:** 1479–1481.
12. Ojha, A., and G. Hatfull. 2007. The role of iron in Mycobacterium smegmatis biofilm formation: the exochelin siderophore is essential in limiting iron conditions for biofilm formation but not for planktonic growth. *Mol. Microbiol.* **66:** 468–483.
13. Niederweis, M. 2003. Mycobacterial porins–new channel proteins in unique outer membranes. *Mol. Microbiol.* **49:** 1167–1177.
14. Stahl, C., S. Kubetzko, I. Kaps, S. Seeber, H. Engelhardt, and M. Niederweis. 2001. MspA provides the main hydrophilic pathway through the cell wall of *Mycobacterium smegmatis. Mol. Microbiol.* **40:** 451–464.
15. Yang, Y., D. Auguin, S. Delbecq, E. Dumas, G. Molle, V. Molle, C. Roumestand, and N. Saint. 2010. Structure of the Mycobacterium tuberculosis OmpATb protein: a model of an oligomeric channel in the mycobacterial cell wall. *Proteins: Structure, Function, and Bioinformatics.* In press.
16. Hall, R., M. Sritharan, A. Messenger, and C. Ratledge. 1987. Iron transport in Mycobacterium smegmatis: occurrence of iron-regulated envelope proteins as potential receptors for iron uptake. *Microbiology.* **133:** 2107.
17. Branton, D., D. Deamer, A. Marziali, H. Bayley, S. Benner, T. Z. Butler, M. Di Ventra, S. Garaj, A. Hibbs, X. Huang, et al. 2008. The potential and challenges of nanopore sequencing. *Nat. Biotechnol.* **26:** 1146–1153.
18. Derrington, I., T. Butler, M. Collins, E. Manrao, M. Pavlenok, M. Niederweis, and J. Gundlach. 2010. Nanopore DNA sequencing with MspA. *Proc. Natl. Acad. Sci. USA.* **107:** 16060–16065.
19. Akeson, M., D. Branton, J. J. Kasianowicz, E. Brandin, and D. W. Deamer. 1999. Microsecond time-scale discrimination among polycytidylic acid, polyadenylic acid, and polyuridylic acid as homopolymers or as segments within single RNA molecules. *Biophys. J.* **77:** 3227–3233.
20. Butler, T. Z., J. H. Gundlach, and M. A. Troll. 2006. Determination of RNA orientation during translocation through a biological nanopore. *Biophys. J.* **90:** 190–199.
21. Barry, C. E. 3rd, R. Lee, K. Mdluli, A. Sampson, B. Schroeder, R. Slayden, and Y. Yuan. 1998. Mycolic acids: structure, biosynthesis and physiological functions. *Prog. Lipid Res.* **37:** 143–179.
22. Butler, T., M. Pavlenok, I. Derrington, M. Niederweis, and J. Gundlach. 2008. Single-molecule DNA detection with an engineered MspA protein nanopore. *Proc. Natl. Acad. Sci. USA.* **105:** 20647–20652.
23. White, S. 1970. A study of lipid bilayer membrane stability using precise measurements of specific capacitance. *Biophys. J.* **10:** 1127–1148.
24. Garcia-Manyes, S., G. Oncins, and F. Sanz. 2005. Effect of ion-binding and chemical phospholipid structure on the nanomechanics of lipid bilayers studied by force spectroscopy. *Biophys. J.* **89:** 1812–1826.

25. Garcia-Manyes, S., G. Oncins, and F. Sanz. 2005. Effect of temperature on the nanomechanics of lipid bilayers studied by force spectroscopy. *Biophys. J.* **89:** 4261–4274.
26. Hirano-Iwata, A., K. Aoto, A. Oshima, T. Taira, R. Yamaguchi, Y. Kimura, and M. Niwano. 2010. Free-standing lipid bilayers in silicon chips-membrane stabilization based on microfabricated apertures with a nanometer-scale smoothness. *Langmuir.* **26:** 1949–1952.
27. White, R., E. Ervin, T. Yang, X. Chen, S. Daniel, P. Cremer, and H. White. 2007. Single ion-channel recordings using glass nanopore membranes. *J. Am. Chem. Soc.* **129:** 11766–11775.
28. Biltonen, R., and D. Lichtenberg. 1993. The use of differential scanning calorimetry as a tool to characterize liposome preparations. *Chem. Phys. Lipids.* **64:** 129–142.
29. Liu, J., C. Barry, G. Besra, and H. Nikaido. 1996. Mycolic acid structure determines the fluidity of the mycobacterial cell wall. *J. Biol. Chem.* **271:** 29545.
30. Liu, J., and H. Nikaido. 1999. A mutant of *Mycobacterium smegmatis* defective in the biosynthesis of mycolic acids accumulates meromycolates. *Proc. Natl. Acad. Sci. USA.* **96:** 4011.
31. Wang, L., R. Slayden, C. Barry, and J. Liu. 2000. Cell wall structure of a mutant of *Mycobacterium smegmatis* defective in the biosynthesis of mycolic acids. *J. Biol. Chem.* **275:** 7224.
32. Paula, S., A. Volkov, A. Van Hoek, T. Haines, and D. Deamer. 1996. Permeation of protons, potassium ions, and small polar molecules through phospholipid bilayers as a function of membrane thickness. *Biophys. J.* **70:** 339–348.
33. Garcia-Manyes, S., and F. Sanz. 2010. Nanomechanics of lipid bilayers by force spectroscopy with AFM: a perspective. *Biochim. Biophys Acta-Biomembranes.* **1798:** 741–749.
34. Joan, M., G. R. Boggs, and K. M. Koshy. 1986. Effect of hydrogen-bonding and non-hydrogen-bonding long chain compounds on the phase transition temperatures of phospholipids. *Chem. Phys. Lipids.* **40:** 23–34.
35. Lundbaek, J. 2008. Lipid bilayer-mediated regulation of ion channel function by amphiphilic drugs. *J. Gen. Physiol.* **131:** 421.
36. Song, H., R. Sandie, Y. Wang, M. Andrade-Navarro, and M. Niederweis. 2008. Identification of outer membrane proteins of Mycobacterium tuberculosis. *Tuberculosis (Edinb.).* **88:** 526–544.